Passivation mechanism in CdTe solar cells: The hybrid role of Se

Selva Chandrasekaran Selvaraj, Sameer Gupta, Damien Caliste, Pascal Pochet

Applied Physics Letters

Passivation mechanism in CdTe solar cells: The hybrid role of Se

Cite as: Appl. Phys. Lett. **119**, 062105 (2021); https://doi.org/10.1063/5.0058290
Submitted: 28 May 2021 . Accepted: 25 July 2021 . Published Online: 10 August 2021

Selva Chandrasekaran Selvaraj, Sameer Gupta, Damien Caliste, et al.

Applied Physics Letters ARTICLE scitation.org/journal/apl

Passivation mechanism in CdTe solar cells: The hybrid role of Se

Cite as: Appl. Phys. Lett. **119**, 062105 (2021); doi: 10.1063/5.0058290
Submitted: 28 May 2021 · Accepted: 25 July 2021 ·
Published Online: 10 August 2021

View Online Export Citation CrossMark

Selva Chandrasekaran Selvaraj, Sameer Gupta, Damien Caliste, and Pascal Pochet[a)]

AFFILIATIONS

Department of Physics, IriG, University Grenoble Alpes and CEA, F-38000 Grenoble, France

[a)]Author to whom correspondence should be addressed: pascal.pochet@cea.fr

ABSTRACT

In this Letter, we report on the role of Se incorporation in the increased efficiency recently measured in Se alloyed cadmium telluride (CdTe) absorbers. This is done by means of density functional theory calculations following an extensive exploration of all the possible diffusion paths of Se. We identify a unique two-step mechanism that accounts for bulk diffusion of chalcogenide interstitials in CdTe, explaining the Se diffusion measured in experiments. The interaction of the diffusing interstitial with the Cd vacancy and the Te antisite is further analyzed in order to understand the passivation of these two main non-radiative recombination centers. Taking into account the approach path of Se, we identify nine complexes that present different levels of passivation. The lowest formation energy is achieved for a ⟨100⟩ Te dimer with two Se in the first neighbor shell. This defect also presents the shallowest donor character defect state due to the presence of Se. This highlights the hybrid role of Se in the mechanism of increased efficiency: it first mediates the diffusion of chalcogenide toward the non-radiative recombination centers before it leads with Te to their optimal passivation. This comprehensive insight should allow further improvements in CdTe-based technologies.

Cadmium telluride (CdTe) solar cells are still at the front end of the few thin film technologies exceeding 22% of efficiency.[1] The latter record was made possible by Se alloying in the CdTe absorber.[2] Se addition is also known to improve X and gamma ray detectors based on CdZnTe.[3] Se alloying results in a bandgap grading from 1.46 to 1.36 eV, leading to an increase in the wavelengths absorption range.[2,4,5] Recent *ab initio* studies based on Density Functional Theory (DFT) confirm this bandgap reduction range for the incorporation of Se up to 35% in CdTe.[6,7]

However, this bandgap reduction does not capture its own reported efficiency improvement. This puzzle was recently solved by means of cathodoluminescence experiments coupled with second ion mass spectroscopy (SIMS) measurements[8] that revealed long-range diffusion of Se into the CdTe absorber as well as a passivation of some critical defects leading to higher luminescence efficiency and longer diffusion lengths. Although these two steps of Se-enhanced efficiency in CdTe are well supported at the microscopic scale, the underlying atomistic mechanism remains hypothetical. Two diffusion types are identified: a pipe diffusion via the grain boundaries and a bulk diffusion inside the grains. The pipe diffusion and the passivation of the grain boundaries has been recently understood at the atomic scale.[9–12] However, for the bulk diffusion, neither the diffusion mechanism of Se nor the detailed passivation scheme by Se has been described so far.

Previous experimental observations[13,14] and DFT based calculations[15–17] consistently propose the Te-antisite and Cd-vacancy as plausible non-radiative recombination centers in CdTe. The former antisite adopts a C_{3v} symmetry and displays a deep donor character represented by a doubly occupied electronic state deep in the bandgap.[15,18] The latter vacancy was expected to be a major acceptor defect in CdTe for almost three decades,[13,19] although a comprehensive mechanism behind its recombination activity was only resolved very recently.[20] In its neutral state, the vacancy can adopt two different topologies: *i*/a C_{2v} symmetry characterized by the formation of a ⟨110⟩ Te dimer, and *ii*/a T_d symmetry stabilized by localized holes. Although both configurations have been identified as important for the recombination process,[20] only the T_d symmetry with the two singly occupied defect states in the bandgap points to an electronic active acceptor character.

In this work, we scrutinize the possible interstitial diffusion of Se to passivate the two aforementioned critical defects. While most of the known diffusion mechanisms in the zinc blende lattice[21–23] failed to reproduce a long range diffusion at intermediate temperature, we propose and assess a two-step mechanism that supports the observed bulk

diffusion.[8] Next, we consider the interaction of the diffusing Se when approaching Cd vacancies or Te anti-site defects. This allows us to identify nine different configurations arising from the bulk diffusion of Se. Among them, we find a unique configuration characterized by a Te dimer on the Cd site that accounts for the passivation of both critical defects.

The numerical investigations have been done using the density functional theory. Since we aim to understand how to passivate the Cd vacancy in its electrically active structure (i.e., the T_d symmetry), all calculations have been done using the local density approximation (LDA). Indeed, this functional is known to give the T_d symmetry as the most stable structure.[24] Valence electrons of Cd (12 e^-, including semi-cores), Te (6 e^-), and Se (6 e^-) were described on a wavelet basis set and core electrons were frozen in the approximation of pseudo-potentials using Hartwigsen–Goedecker–Hutter[25] formalism using BigDFT-code.[26] The calculated value of the CdTe lattice constant for these pseudo-potentials is 6.42 Å, which is close to the experimental value of 6.48 Å.[27] All the defects presented in Fig. 1 have been obtained from geometry relaxations[28] in 216-atom super-cells of CdTe in $F\bar{4}3m$ space group. Barrier energies in Fig. 2 were obtained with the nudged elastic band (NEB) method in 64-atom super-cells, while the top-most configuration was later relaxed in 216-atom super-cells.

Fiducia *et al.*[8] have shown that the selenium first concentrates at the grain boundaries before fast diffusing inside the core of the CdTe grains. Once inside the CdTe, the selenium can be present as a substitutional atom or on an interstitial position. In the latter case, we have enumerated all the possible interstitial sites for zinc blende semiconductors, including tetrahedral, hexagonal, or various split positions. The interstitial atom interacting with a regular site atom and pushing it to create bond such that the two are symmetrically displaced from regular site is considered as split position.[29,30] It appears that only split along ⟨110⟩ directions on Te sites present low energies, while split along ⟨100⟩ directions are the most favorable positions for Cd sites, respectively. The split configuration along a given direction corresponds to a lattice site that is shared by two atoms oriented in the given direction as depicted in Fig. 1, panel (a) and (b). Similar observation about the stability of split configuration of Te self-interstiitial was

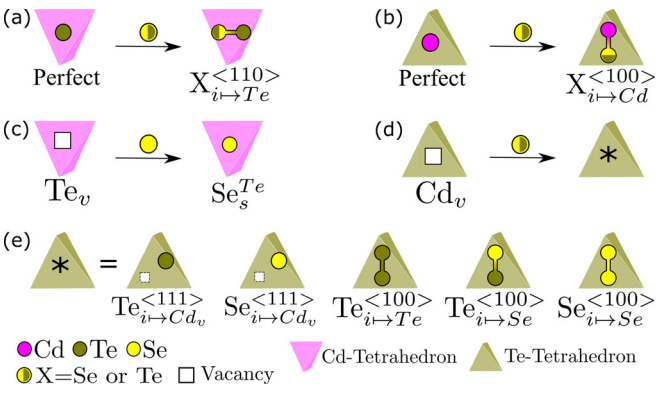

FIG. 1. (a)–(c) Main topologies of defects including selenium, tellurium, and cadmium. Pink tetrahedrons display the tetrahedrons formed by four Cd atoms. In perfect CdTe, the centers of such tetrahedrons are occupied by tellurium. Respectively, greenish tetrahedrons stand for Te neighbors of a Cd atom. Panel (e) five main passivated structures of the cadmium vacancy shown in panel (d).

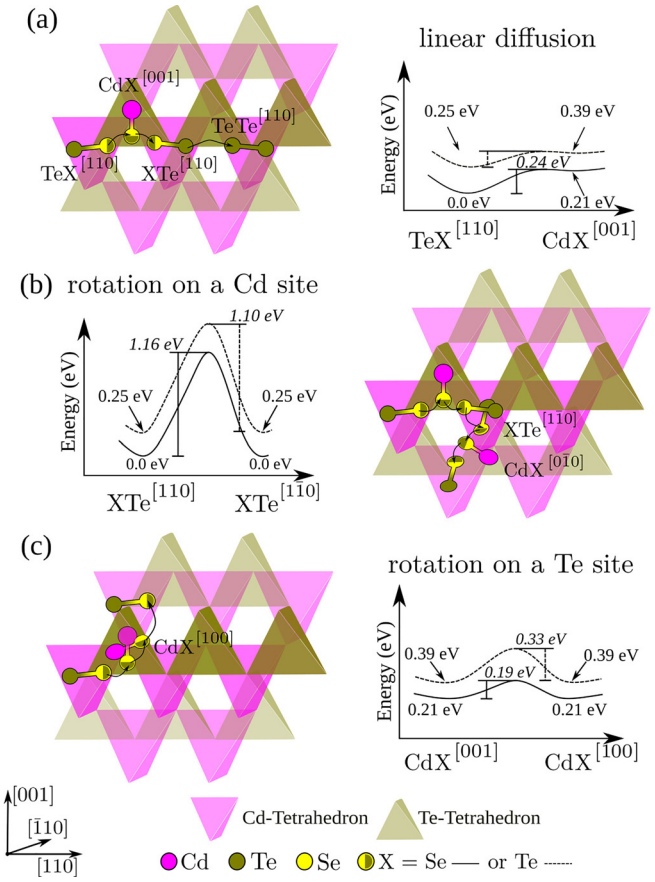

FIG. 2. (a)–(c) are pictorial representations of chalcogenide diffusion paths in bulk CdTe constituted by Cd (pink) and Te (greenish) tetrahedrons. Panel (a) corresponds to a series of two consecutive linear diffusion steps at the first neighbor tetrahedron leaving the Se in the intermediate tetrahedron. While in panel (b) and (c), an intermediate rotation step allows to keep Se as a diffusion species (see the text). In all panels, energy profiles corresponding to Se (plain line) and Te (dashed line) diffusion are given. Absolute formation energy of stable configurations is given in normal font and are referenced to the TeSe [110] split intestitial, while barriers linking two stable configurations are provided in italic fonts.

made by Du *et al.*[30] Selenium can also kick out a cadmium or a tellurium atom and come to occupy a substitutional position, creating an anti-site when sitting inside a tetrahedron of Te atoms, or as a substitution in the complementary Cd tetrahedron [see Fig. 1(c)].

To compare the energetics of all these defects including a various number of atoms per species, we have used a standard formation energy formulation where the total energy of a defected super-cell is reduced by the number of the constituent species times their respective chemical potentials.[21,31] We need to define three references (i.e., chemical potentials) for the three Cd, Te, and Se species. We define the chemical potential of the Cd–Te pair using the CdTe bulk. Since we want to describe crystals grown in Te-rich conditions where the Cd-vacancies are constitutional defects, we chose to use the Cd-vacancy super-cell to complement the Cd–Te pair chemical potential definition and set up a chemical potential value for the two species. We thus use CdTe bulk and Cd vacancy as reference and put their formation

energy to zero, defining like that a chemical potential for cadmium species and tellurium species. In addition, since the selenium is entering the CdTe crystal as an interstitial, we decide to take the selenium defect within a perfect CdTe super-cell with the lower energy as the reference, namely, the split SeTe ⟨110⟩ in a Cd-tetrahedron [see Fig. 1(a)]. This defines the chemical potential for selenium. Within this framework, other possible selenium configurations are less favorable: a selenium split interstitial on a Cd site [Fig. 1(b)] is 0.21 eV higher in energy, while a tellurium split on a Te site with a non-interacting substitutional Se on a Te site [kick-out mechanism, Figs. 1(a) and 1(c)] is also 0.26 eV higher in energy [reduced to 0.22 eV when the substitutional selenium is first neighbor of the split TeTe ⟨110⟩ as in Fig. 1(e)]. Other interstitial defects are much higher in energy, like the hexagonal interstitial at the Te site (1.27 eV) and the tetrahedral interstitial at the Cd site (1.62 eV).

Having investigated the energetic landscape for selenium positions within CdTe crystal, it remains to describe its diffusion. CdTe being a binary semiconductor complicates this movement since available nearby atoms will change their chemical nature at each step. In addition, since the Se split interstitial is not a self-interstitial, it cannot diffuse simply by switching its position with nearby atom and do it again.[23] It also requires some additional step to avoid getting trapped at a substitutional site. We have found three possible movements of low energy starting from a selenium in split ⟨110⟩ interstitial positioned in a Cd-tetrahedron.

The first step is to simply move the selenium along the [110] direction, thus creating another Se–Te [110] split in the first neighbor Cd-tetrahedron [left end-side in Fig. 2(a)]. In the latter configuration, the respective positions of Se and Te in the split are swapped with respect to the ones in the initial configuration. An equivalent movement is likely for the tellurium atom in the split interstitial, where it can itself leave the Se–Te split position to create a [110] split interstitial made of two Te atoms [right-most Te–Te split in Fig. 2(a)]. This movement ends up leaving the selenium as a substitution on a Te site and mainly immobile in the lattice, while the Te interstitial can continue its linear diffusion along the [110] direction. The migration barriers for this linear diffusion path are 0.24 and 0.14 eV for mixed Se–Te and pure Te split interstitial, respectively. The tellurium interstitials diffuse faster than the selenium ones in a linear direction. To actually achieve long-range diffusion for Se in volume, a rotation step is required. A direct rotation step of the Te–Se [110] split in a Cd-tetrahedron [see Fig. 2(b)] where it is the most stable would allow long range diffusion of the selenium by accessing diffusion along other directions of the ⟨110⟩ family like [101] or [011]. However, the energy barrier for the corresponding rotation is 1.16 eV and is relatively very high in comparison to linear diffusion barrier. It is notable that the same on-site rotation of a Te–Te [110] split is also around 1.10 eV. Nonetheless, there is an additional possibility for rotation. Indeed, during the linear diffusion, an intermediate [001] Cd–Se split is created in a Te-tetrahedron [see Fig. 2(a)]. A rotation at this intermediate state allows to obtain the final [110] Te–Se split in an orientation, permitting further diffusion of Se [see Fig. 2(c)]. The associated rotation barrier for Cd–Se split interstitial is 0.19 eV, putting the overall barrier for the rotation of a Te–Se split interstitial at 0.40 eV. On the contrary, such a rotation for the [001] Cd–Te split is less likely with a barrier of 0.33 eV, making the full diffusion process of Te interstitials in volume through linear and re-orientation mechanism around 0.47 eV. For the sake of completeness, we have also calculated barriers linking hexagonal and tetrahedral interstitial positions. Such diffusion paths are much simpler since they would allow a direct diffusion of the selenium atom in the CdTe bulk. However, the corresponding barriers for both chalcogenides Se and Te are $\geq$1 eV and therefore, such diffusion of pure chalcogenide interstitials are not favorable.

To summarize, a mix of translation and rotation movements present the lower migration energy for Se diffusion. They occur with a rate based on a barrier of 0.24 eV for the linear diffusion and a barrier of 0.40 eV for the reorientation. The other possible defect configurations or even diffusion paths calculated in this Letter present higher combinations of formation and activation energies. The differences in energies with the lowest mechanism proposed here are large enough for the other mechanisms to be happen in a negligible rate compared to the lowest energy one at the temperature considered in Fiducia's article.[8] Of course, it is also possible for the selenium to leave the split and be stuck as a substitutional while tellurium continues to diffuse by itself. Tellurium interstitial atoms, without the presence of selenium atoms, follow the same kind of translation-rotation mechanisms, but with a different rate between linear diffusion (0.14 eV) and reorientation steps (0.47 eV). The linear diffusion will be predominent over the possibility to reorientate, leading to a quick disappearance of Te interstitial atoms on interfaces or grain boundaries. On the contrary, the selenium moderates the Te diffusion, allowing both species to diffuse as a pair and giving them the possibility to explore a wide volume of the CdTe grains. Thus, Se is mandatory to allow these impurities to reach critical defects such as a Cd vacancy.

Next, using the topology of the approaching paths, we investigate the possible reactions leading to the passivation of the electronic levels created by a Cd vacancy [see Fig. 3(a)]. The simplest interaction would be for the selenium to come and create a substitution at the vacancy site. The resulting position is equivalent to an anti-site where the selenium is displaced within a Te tetrahedron face adopting a C_{3v} symmetry as for the Te anti-site. Different chemistry will be achieved depending on the orientation of the entering split interstitial [small pink tetrahedron on the left panels in Fig. 3(b)].

In all final configurations, the chalcogenide atom is displaced along a ⟨111⟩ direction inside the vacancy. With respect to the choice of our chemical potentials, the formation energies of these anti-sites are negative, so that all of them are thermodynamically stable complexes over the Cd-vacancy constitutional defect. Nonetheless, it is possible to create even more stable configurations than these mono-passivated complexes. Indeed, the displacement of the chalcogenide anti-site atom along the ⟨111⟩ direction inside the vacancy leaves a dangling bond that could be passivated by a second chalcogenide approaching the vacancy site. As a result, a second interstitial can come into play and create a ⟨001⟩ split defect inside the vacancy, see Fig. 3(c). These bi-passivated configurations have further lower formation energy in comparison to mono-passivated configurations. We have consistently calculated configurations where one or two selenium atoms passivate the Cd vacancy, directly or as first neighbors. This leads to nine unique configurations derived from the nature of the involved split chalcogenide and its approaching path inside the vacancy. The reactions following the last diffusion step are depicted in Fig. 3(c). The most stable defect of the series is found to be a ⟨001⟩ Te dimer on a Cd site with two selenium atoms in the first neighbors shell. This configuration is reminiscent with the recently proposed Te

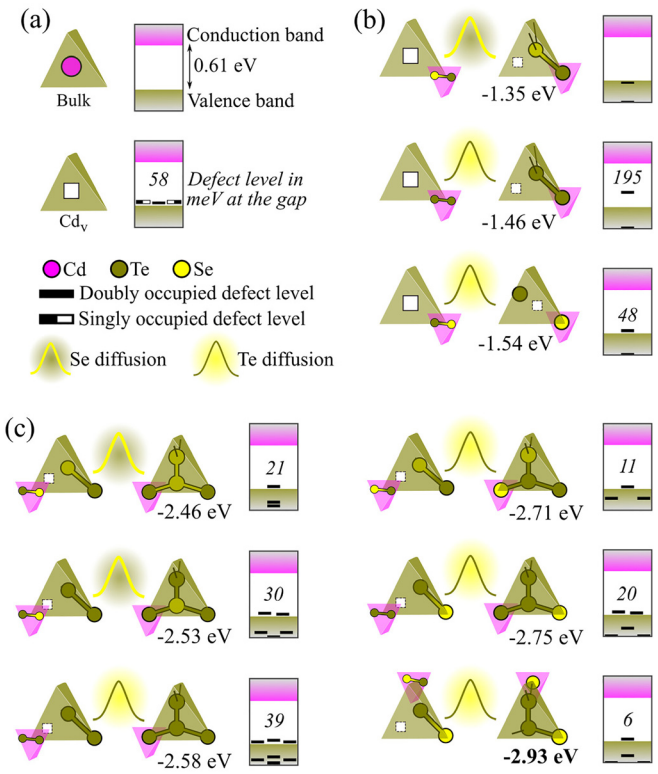

FIG. 3. (a) Simplified electronic structures of bulk CdTe and Cd_v. (b) Partially passivated Cd_v by X (= Se or Te) from a nearest $X_{i\to X}^{\langle 110\rangle}$ defect. (c) Full passivation of partially passivated Cd_v by X from a nearest $X_{i\to X}^{\langle 110\rangle}$ defect. Defect formation energies are given for all the configurations in (b) and (c) and their electronic structures of defects levels with respect to bulk valence and conduction bands are in the corresponding side panel of each defect configuration. Relative position of defect energy levels measured from the VBM in meV is shown in bandgap. The type of chalcogenide atom involved in the last diffusion step is coded by a greenish or yellow barrier symbol, while its exact topology is described inside the small pink tetrahedron for all complexes reactions in panels (b) and (c).

interstitial-antisite complex[32] where the additional presence of Se decreases the formation energy by 0.35 eV [bottom configurations in Fig. 3(c)].

Having the formation energies for the nine complexes reported in Figs. 3(b) and 3(c) gives an idea of their relative concentrations in a sample where an isotropic diffusion of chalcogenide atoms has been promoted by Se. A rough estimate of the formation energy is given by the number of passivated dangling bond: $\simeq -1.4$ and $\simeq -2.6$ eV for the mono- and the bi-passivated configurations, respectively. To get more insight, the electronic band structure of all nine complexes is analyzed to characterize the deep electronic defect states in the bulk bandgap of CdTe. In order to focus the discussion, we report a simplified band structure [right end side in Figs. 3(a)–3(c)] where the defect electronic states appear within the bandgap.

The calculated bulk bandgap of CdTe is 0.61 eV, which is in good agreement with previous calculations[33] although it is considerably underestimated when compared to experimental values. This bandgap error is well documented[34] and derived from the use of the LDA functional. We assume it will not change our conclusions because we are focusing on occupation of defect states close to the valence band and not to their exact position with respect to band edges. When a cadmium vacancy is present in bulk CdTe, it leaves the surrounding Te atoms in the T_d symmetry of the crystal with six electrons from the four dangling bonds. In the relaxed ground state T_d symmetry structure, two electrons out of these six electrons occupy a state lying deep in the valence band (not shown), while the rest four electrons occupy two degenerated singly occupied states and one doubly occupied state at 58 and 38 meV from valence band maximum (VBM), respectively [Fig. 3(a)]. The two singly occupied states leave space to accommodate for two electrons and are responsible for the deep non-radiative acceptor character of Cd_v that reduces the cell performance by increasing recombination.

In the case of the mono-passivated Cd vacancy [Fig. 3(b)], there is not anymore singly occupied levels in the bandgap. Still a dangling bond is left behind in all three configurations characterized by doubly occupied anti-bonding states. The Te-antisite has the corresponding state deep in the bandgap at 195 meV above VBM. This defect state is responsible for the non-radiative activity of the Te-antisite. The position of defect state is in the line with previous LDA studies.[35] For both the mono-passivated configurations alloyed with one Se atom, the energy of the anti-bonding state is significantly lowered close to VBM. This lowering is derived from the reduction in anti-bonding interaction and the anion-anion repulsion between the Se atom and Te atoms due to an electronegativity difference as deduced from the Kohn–Sham eigen state plots (not shown). More precisely, for the ground state of the series (i.e., a Te anti-site with a Se align along the C_3 axis), the anti-bonding state lies at 48 meV above VBM. This lowering of 147 meV is consistent with more precise GW calculations[15] that gives a lowering of 130 meV. Finally, the anti-bonding state moves further lower in energy below VBM for the last configuration of the series where the Se atom is in anti-site position. The two latter configurations with one Se atom display weak anti-bonding interaction and defect states lying close to VBM, significantly reducing hole-trapping probability. Both are thus expected to be tolerant for solar applications and enhance radiative recombination.[15,36] Worth is noticing that the three *mono-passivated* vacancy configurations will coexist as the final configuration strongly derived from the nature of approaching split interstitial.

Next, we consider the further reaction of this three configurations with a second diffusing chalcogenide split interstitial that leads to six possible configurations where the vacancy is occupied by two chalcogenides, as shown on Fig. 3(c). All configurations adopt a $\langle 001\rangle$ chalcogenide dimer topology with different chemistry in the dimer and in the first shell as a result of the exact nature of the diffusing chalcogenide involved in the two consecutive passivation steps. The dimer topology is characterized by a strong bonding character state between the two chalcogenide atoms inside the vacancy and the absence of dangling bond for the six configurations. Yet, the defect level stay close to the VBM within 40 meV with no defect state lying deep in the bandgap for all of them. In other words, all these *bi-passivated* configurations rectify the defect states of both Cd vacancy and Te antisite that otherwise are detrimental for solar applications.

To summarize, we have calculated the diffusion mechanism of Se in CdTe allowing us to probe the interaction of Se with detrimental defects. We have demonstrated by means of DFT calculations that the

cadmium vacancy in CdTe can be efficiently passivated by a pairing with one or two chalcogenide atoms. The created bonds within the vacancy ensure that no singly occupied levels remains within the bandgap, neutralizing any recombination effect in the passivated vacancy. The lowest energy defect in Te-rich conditions in the presence of selenium impurities consists of a ⟨001⟩ Te-dimer on a Cd site with two Se atoms in the first neighbor shell. The five other combinations also present the same kind of passivating effect. Due to the diffusion driven passivation mechanism, we expect that all configuration can co-exist. The role of Se in this passivation mechanism is, thus, a hybrid one. First, Se moderates the fast and linear diffusion of Te, thus enabling both chalcogenide atoms to diffuse in the volume and reach Cd-vacancies or Te anti-sites. Second, the peculiar diffusion mechanism promotes Se alloying in the first shell of the Te dimer that improves the tolerance of the latter. This comprehensive insight into the role of Se in the passivation mechanism of CdTe absorbers should allow further improvements alongside other doping strategies[37,38] to take efficiencies in the range of 25% in the coming years.[39]

AUTHORS' CONTRIBUTIONS

S.C.S. and S.G. contributed equally to this work.

We acknowledge partial financial support from the Mechaspin Project (No. ANR-17-CE24–0024). The BigDFT calculations were done using the French supercomputers (GENCI) through Project No. 6107. D.C. also acknowledged GPU hours in the framework of the *Grands Challenges* Jean Zay 2020 (IDRIS No. 100960).

DATA AVAILABILITY

The data that support the findings of this study are available from the corresponding author upon reasonable request.

REFERENCES

[1]M. Powalla, S. Paetel, E. Ahlswede, R. Wuerz, C. D. Wessendorf, and T. Magorian Friedlmeier, "Thin–film solar cells exceeding 22% solar cell efficiency: An overview on $CdTe^{-}$, $Cu(In,Ga)Se^{2-}$, and perovskite-based materials," Appl. Phys. Rev. **5**, 041602 (2018).
[2]N. R. Paudel and Y. Yan, "Enhancing the photo-currents of CdTe thin-film solar cells in both short and long wavelength regions," Appl. Phys. Lett. **105**, 183510 (2014).
[3]S. K. Chaudhuri, M. Sajjad, J. W. Kleppinger, and K. C. Mandal, "Charge transport properties in CdZnTeSe semiconductor room-temperature γ-ray detectors," J. Appl. Phys. **127**, 245706 (2020).
[4]A. H. Munshi, J. Kephart, A. Abbas, J. Raguse, J.-N. Beaudry, K. Barth, J. Sites, J. Walls, and W. S. Sampath, "Polycrystalline CdSeTe/CdTe absorber cells with 28 mA/cm^2 short-circuit current," IEEE J. Photovoltaics **8**, 310–314 (2018).
[5]M. Lingg, A. Spescha, S. G. Haass, R. Carron, S. Buecheler, and A. N. Tiwari, "Structural and electronic properties of $CdTe_{1-x}Se_x$ films and their application in solar cells," Sci. Technol. Adv. Mater. **19**, 683–692 (2018).
[6]J. Yang and S.-H. Wei, "First-principles study of the band gap tuning and doping control in $CdSe_xTe_{1-x}$ alloy for high efficiency solar cell," Chin. Phys. B **28**, 086106 (2019).
[7]M. J. Watts, T. A. M. Fiducia, B. Sanyal, R. Smith, J. M. Walls, and P. Goddard, "Enhancement of photovoltaic efficiency in $CdSe_xTe_{1x}$ (where $0 \leqslant x \leqslant 1$): Insights from density functional theory," J. Phys.: Condens. Matter **32**, 125702 (2020).
[8]T. A. M. Fiducia, B. G. Mendis, K. Li, C. R. M. Grovenor, A. H. Munshi, K. Barth, W. S. Sampath, L. D. Wright, A. Abbas, J. W. Bowers, and J. M. Walls, "Understanding the role of selenium in defect passivation for highly efficient selenium-alloyed cadmium telluride solar cells," Nat. Energy **4**, 504–511 (2019).
[9]X. Zheng, D. Kuciauskas, J. Moseley, E. Colegrove, D. S. Albin, H. Moutinho, J. N. Duenow, T. Ablekim, S. P. Harvey, A. Ferguson, and W. K. Metzger, "Recombination and bandgap engineering in CdSeTe/CdTe solar cells," APL Mater. **7**, 071112 (2019).
[10]C.-J. Tong and K. P. McKenna, "Passivating grain boundaries in polycrystalline CdTe," J. Phys. Chem. C **123**, 23882–23889 (2019).
[11]J. Guo, A. Mannodi-Kanakkithodi, F. G. Sen, E. Schwenker, E. S. Barnard, A. Munshi, W. Sampath, M. K. Y. Chan, and R. F. Klie, "Effect of selenium and chlorine co-passivation in polycrystalline CdSeTe devices," Appl. Phys. Lett. **115**, 153901 (2019).
[12]R. Wang, M. Lan, and S.-H. Wei, "Enhanced performance of Se-alloyed CdTe solar cells: The role of Se-segregation on the grain boundaries," J. Appl. Phys. **129**, 024501 (2021).
[13]C. Szeles, Y. Y. Shan, K. G. Lynn, A. R. Moodenbaugh, and E. E. Eissler, "Trapping properties of cadmium vacancies in $Cd_{1-x}Zn_xTe$," Phys. Rev. B **55**, 6945–6949 (1997).
[14]C. Li, X. Hao, Y. He, J. Zhang, L. Wu, W. Li, W. Wang, L. Feng, I. M. Monirul, K. Akimoto, and T. Sakurai, "Identification of deep level defects in CdTe solar cells using transient photo-capacitance spectroscopy," Jpn. J. Appl. Phys., Part 1 **60**, SBBF01 (2021).
[15]M. A. Flores, W. Orellana, and E. Menéndez-Proupin, "First-principles DFT + GW study of the Te antisite in CdTe," Comput. Mater. Sci. **125**, 176–182 (2016).
[16]J.-H. Yang, W.-J. Yin, J.-S. Park, J. Ma, and S.-H. Wei, "Review on first-principles study of defect properties of CdTe as a solar cell absorber," Semicond. Sci. Technol. **31**, 083002 (2016).
[17]S.-H. Wei and S. B. Zhang, "Chemical trends of defect formation and doping limit in II-VI semiconductors: The case of CdTe," Phys. Rev. B **66**, 155211 (2002).
[18]J.-H. Yang, L. Shi, L.-W. Wang, and S.-H. Wei, "Non-radiative carrier recombination enhanced by two-level process: A first-principles study," Sci. Rep. **6**, 2045–2322 (2016).
[19]P. Emanuelsson, P. Omling, B. K. Meyer, M. Wienecke, and M. Schenk, "Identification of the cadmium vacancy in CdTe by electron paramagnetic resonance," Phys. Rev. B **47**, 15578–15580 (1993).
[20]S. R. Kavanagh, A. Walsh, and D. O. Scanlon, "Rapid recombination by cadmium vacancies in CdTe," ACS Energy Lett. **6**, 1392–1398 (2021).
[21]D. Caliste, P. Pochet, T. Deutsch, and F. Lançon, "Germanium diffusion mechanisms in silicon from first principles," Phys. Rev. B **75**, 125203 (2007).
[22]J. Roehl and S. Khare, "Diffusion of Te vacancy and interstitials of Te, Cl, O, S, P and Sb in CdTe: A density functional theory study," Sol. Energy Mater. Sol. Cells **128**, 343–350 (2014).
[23]J. Ma, J. Yang, S.-H. Wei, and J. L. F. Da Silva, "Correlation between the electronic structures and diffusion paths of interstitial defects in semiconductors: The case of CdTe," Phys. Rev. B **90**, 155208 (2014).
[24]A. Carvalho, A. K. Tagantsev, S. Öberg, P. R. Briddon, and N. Setter, "Cation-site intrinsic defects in Zn-doped CdTe," Phys. Rev. B **81**, 075215 (2010).
[25]C. Hartwigsen, S. Gœdecker, and J. Hutter, "Relativistic separable dual-space Gaussian pseudopotentials from H to Rn," Phys. Rev. B **58**, 3641 (1998).
[26]S. Mohr, L. E. Ratcliff, L. Genovese, D. Caliste, P. Boulanger, S. Goedecker, and T. Deutsch, "Accurate and efficient linear scaling DFT calculations with universal applicability," Phys. Chem. Chem. Phys. **17**, 31360–31370 (2015).
[27]A. J. Strauss, "The physical properties of cadmium telluride," Rev. Phys. Appl. **12**, 167–184 (1977).
[28]E. Bitzek, P. Koskinen, F. Gähler, M. Moseler, and P. Gumbsch, "Structural relaxation made simple," Phys. Rev. Lett. **97**, 170201 (2006).
[29]R. J. Needs, "First-principles calculations of self-interstitial defect structures and diffusion paths in silicon," J. Phys.: Condens. Matter **11**, 10437–10450 (1999).
[30]M.-H. Du, H. Takenaka, and D. J. Singh, "Native defects and oxygen and hydrogen-related defect complexes in CdTe: Density functional calculations," J. Appl. Phys. **104**, 093521 (2008).
[31]C. Freysoldt, B. Grabowski, T. Hickel, J. Neugebauer, G. Kresse, A. Janotti, and C. G. Van de Walle, "First-principles calculations for point defects in solids," Rev. Mod. Phys. **86**, 253–305 (2014).
[32]D. Krasikov and I. Sankin, "Defect interactions and the role of complexes in the CdTe solar cell absorber," J. Mater. Chem. A **5**, 3503–3513 (2017).

[33]A. Lindström, S. Mirbt, B. Sanyal, and M. Klintenberg, "High resistivity in undoped CdTe: Carrier compensation of Te antisites and Cd vacancies," J. Phys. D: Appl. Phys. **49**, 035101 (2016).
[34]J. P. Perdew, "Density functional theory and the band gap problem," Int. J. Quantum Chem. **28**, 497–523 (2009).
[35]A. Shepidchenko, S. Mirbt, B. Sanyal, A. Håkansson, and M. Klintenberg, "Tailoring of defect levels by deformations: Te-antisite in CdTe," J. Phys.: Condens. Matter **25**, 415801 (2013).
[36]M. A. Flores, W. Orellana, and E. Menéndez-Proupin, "First-principles DFT + *gw* study of oxygen-doped CdTe," Phys. Rev. B **93**, 184103 (2016).
[37]A. H. Munshi, J. M. Kephart, A. Abbas, A. Danielson, G. Glinas, J.-N. Beaudry, K. L. Barth, J. M. Walls, and W. S. Sampath, "Effect of $CdCl_2$ passivation treatment on microstructure and performance of CdSeTe/CdTe thin-film photovoltaic devices," Sol. Energy Mater. Sol. Cells **186**, 259–265 (2018).
[38]S. Paul, S. Sohal, C. Swartz, D.-B. Li, S. S. Bista, C. R. Grice, Y. Yan, M. Holtz, and J. V. Li, "Effects of post-deposition $CdCl_2$ annealing on electronic properties of CdTe solar cells," Sol. Energy **211**, 938–948 (2020).
[39]A. Romeo and E. Artegiani, "CdTe-based thin film solar cells: Past, present and future," Energies **14**, 1684 (2021).